

**COLLISIONAL EVOLUTION OF THE PRIMORDIAL KUIPER BELT, SCATTERED DISK, AND TROJAN POPULATIONS.** W. F. Bottke<sup>1</sup>, R. Marschall<sup>2</sup>, D. Vokrouhlický<sup>3</sup>, D. Nesvorný<sup>1</sup>, A. Morbidelli<sup>2</sup>, R. Deienno<sup>1</sup>, M. Kirchoff<sup>1</sup>, S. Marchi<sup>1</sup>, H. Levison<sup>1</sup>. <sup>1</sup>Southwest Research Institute, Boulder, CO, USA ([bottke@boulder.swri.edu](mailto:bottke@boulder.swri.edu)), <sup>2</sup>Université Côte d’Azur, Observatoire de la Côte d’Azur, CNRS, Laboratoire Lagrange, Nice, France. <sup>3</sup>Institute of Astronomy, Charles University, Prague, Czech Republic.

**Introduction.** The Kuiper belt, scattered disk, Oort cloud, and Jupiter/Neptune Trojans were derived from a primordial Kuiper belt (PKB) that likely once existed beyond 20 au. The end of the PKB was brought about by Neptune migrating through it at some early time, triggering a giant planet instability that led to our system of planets and small bodies [e.g., 1].

Up to now, this scenario has mainly been tested using dynamical models, but enough progress has been made to now consider collisional processes and their constraints. For example, a major challenge for any model is to explain the paucity of primary  $D < 10$ -20 km diameter craters found on Charon, Arrokoth, Europa, and Ganymede [2-3]. Collectively, these crater data indicate the KBO size frequency distribution (SFD) between  $d \sim 30$  m and  $\sim 1$  km is remarkably shallow (i.e., cumulative power law slope of  $q \sim -1$ ) [4].

Here we use *Boulder* [5] to model collisional evolution of PKB/daughter populations. For constraints, we employed (i) crater SFDs on icy satellites and KBOs [e.g., 2-3; 6-7], and (ii) observed SFDs of populations derived from the PKB (e.g., Jupiter’s Trojans) [8-9]. Note that craters on icy satellites allow us to infer the SFD of the PKB population scattered onto planet-crossing orbits as well as those that went to the scattered disk (i.e., source of Centaurs/JFCs).

**Model Setup.** *Boulder* requires several input parameters derived from other models.

First, for the initial SFD of the PKB, we gave it a shape taken from hydrodynamical simulations of the streaming instability (**Fig. 1**) [10]. The initial mass was set to  $\sim 30$  Earth masses; most in  $d \sim 100$  km objects and relatively few in  $d < 100$  km objects. Note that the shape of this SFD is similar to the one predicted for the primordial asteroid belt [11].

Second, we delayed Neptune’s entry into the PKB after the gas disk was eliminated by  $t_{\text{delay}} = 0$  to 50 Myr [1]. Longer values of  $t_{\text{delay}}$  mean more collisional evolution takes place within a massive PKB excited by gravitational perturbations from a distant Neptune and embedded Pluto-sized bodies [4, 10].

Third, dynamical simulations [10] were used to calculate the intrinsic collision probability  $P_i$ , mean impact speed  $V$ , and dynamical depletion values of objects residing within the PKB and those scattered into different daughter populations, such as those reaching giant planet-crossing orbits and those captured as Trojans.

Fourth, for each  $t_{\text{delay}}$ , we tested  $\sim 10^4$  disruption law functions (i.e.,  $Q_D^*$  functions). They define the kinetic energy needed for a projectile to break up a target and  $> 50\%$  of the ejecta away at escape velocity.

**Model Results.** To get a shallow slope between 30 m and 1 km (and other constraints), we had to adopt  $Q_D^*$  functions where the easiest body to disrupt from an energy/mass perspective was  $d_{\text{min}} \sim 20$  m. A model SFD that matches constraints is given in **Fig. 1**.

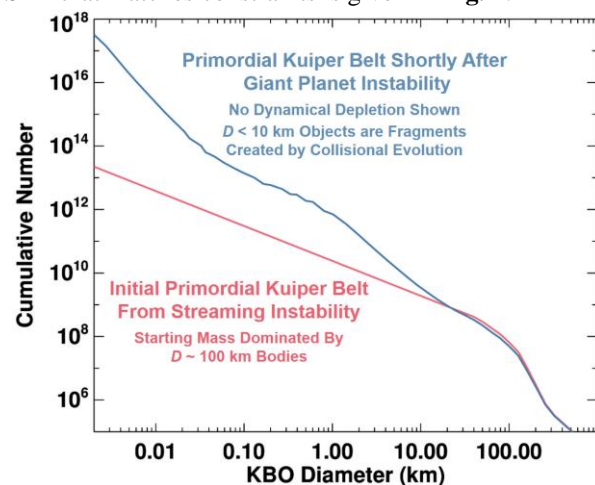


**Fig. 1.** Collisional evolution of primordial Kuiper belt.

The wavy SFD comes from a collisional cascade. Large objects disrupt and create fragments. KBOs with  $d < 20$  m grind into a Dohnanyi SFD with  $q \sim -3$  (a slope that also explains dust observed by New Horizons [4]). This steep SFD decimates  $d > 20$  m objects, leading to  $q \sim -1$  for  $30 \text{ m} < d < 1 \text{ km}$ . In turn, this shallow branch means fewer projectiles exist to disrupt  $d > 1 \text{ km}$  bodies, making a “bump” near  $d \sim 1 \text{ km}$ .

Similar grinding occurs in the main belt, but there  $d_{\text{min}}$  is  $\sim 200$  m [11]. This leads to a similarly-shaped SFD, except  $q \sim -1$  is between  $200 \text{ m} < d < 2 \text{ km}$  and the steeper slope starts at  $d > 2 \text{ km}$  [11]. *This may explain why crater SFDs on icy satellites look like they were made by asteroids; the shape of our model SFD in Fig. 1 is not that different from the main belt SFD.*

Our model also suggests that most  $d < 10$  km bodies are fragments of larger bodies. *This may explain why observed comets often have shapes comparable to similar-sized asteroids.*

Our best-fit model SFDs depends on two coupled parameters:  $t_{\text{delay}}$  and the disruption law of large KBOs. If  $t_{\text{delay}}$  is a few Myr, KBOs disrupt like weak ice from

[12]. If  $t_{\text{delay}}$  is tens of Myr or more, KBOs need to be harder to disrupt and act more like strong ice [e.g., 13].

**Crater/Impactor Results.** Our model SFD from Fig. 1 can be compared to crater SFDs on different icy worlds. For example, primary craters from the Galilean satellites [6] are shown in Fig. 2. Using scaling laws discussed in [2], we find a match between model/crater SFDs. Comparable model/crater SFD plots can be made for most icy satellites and KBOs, provided we stick to craters made by  $d > 1$  km projectiles [2, 7].

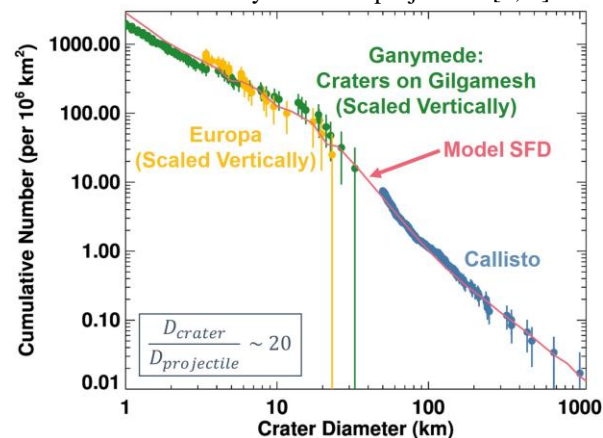


Fig. 2. Primary craters on the Galilean satellites [6].

It is more difficult to match crater SFDs made by  $d < 1$  km projectiles because secondaries/sesquinaries often dominate primary crater populations [3]. Phoebe, however, avoids these issues, with the model SFD reproducing observed craters even at sub-km sizes [7].

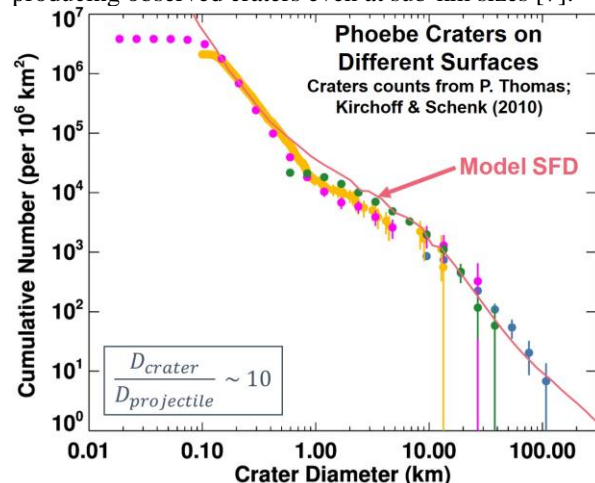


Fig. 3. Phoebe craters counted by different authors.

Our steep SFD at small sizes yields  $\sim 20$   $d > 10$  m impacts on Jupiter per year. This matches the observed rate of superbolide impacts on Jupiter [14].

**Jupiter Trojans.** A potential issue comes from the Jupiter Trojan SFD. Giant planet instability models show Trojans come from the PKB [1], yet the Trojan SFD, with  $q \sim -2$  for  $d < 100$  km bodies, does not

match our model SFD (blue curve vs. black dots in Fig. 4) [8-9]. Trojan collisional evolution over the last  $\sim 4$ -4.5 Gyr is also too limited to fix this problem [8].

The missing component may be collisional evolution taking place prior to Trojan capture. Consider that Neptune's migration sends an enormous number of KBOs from the PKB to  $\sim 5$  au over a short time, where:

- Collision probabilities scale with heliocentric distance  $r$  as  $P_i \sim r^{-3.5}$  [8] so  $P_i$  increases  $(25 \text{ au}/5 \text{ au})^{3.5} \sim 280$  times near 5 au.
- Impact speeds go up ( $\sim 5$  km/s vs.  $\sim 2$ -3 km/s).
- Prior to capture, proto-Trojans evolve for a few Myr within a population that is  $\sim 1\%$  of the PKB.

Our model runs show this burst of collisional evolution can modify the SFD of the proto-Trojans prior to capture, giving them a Trojan-like SFD (Fig. 4).

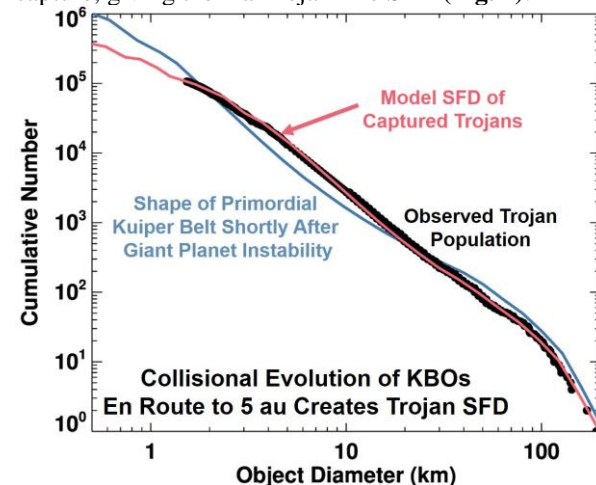


Fig. 4. Collisions create Trojan SFD prior to capture.

**Implications.** In preliminary work, we have combined our model SFDs with dynamical simulations from [8], satellite impact probabilities from [3], and crater scaling laws (e.g., [2]). Our results suggest most ancient surfaces on Saturn's satellites are  $> 4$  Ga. This challenges the idea many moons formed  $< 0.1$  Ga [15].

**References.** [1] Nesvorný, D. 2018. *Annu. Rev. Astro. Astrophys.* **56**, 137. [2] Singer, K., et al. 2019. *Science* **363**, 955. [3] Zahnle, K. et al. 2003. *Icarus* **163**, 263. [4] Morbidelli, A., et al. 2021. *Icarus* **356**, 114256. [5] Morbidelli, A. et al. 2009. *Icarus* **204**, 558. [6] Schenk, P. et al. 2004. In *Jupiter*, 427. [7] Kirchoff, M. & P. Schenk. 2010. *Icarus* **206**, 485. [8] Wong, I. & M. Brown. 2015. *Astron. J.* **150**, 174 [9] Yoshida, F. & T. Terai. 2017. *Astron. J.* **154**, 71. [10] Nesvorný, D., 2018. *Nature Astro.* **2**, 878. [11] Bottke, W. F. et al. 2020. *Astron. J.* **160**, 14. [12] Leinhardt, Z., & Stewart, S. 2009. *Icarus* **675**, 542 [13] Benz, W. and E. Asphaug 1999. *Icarus* **142**, 5. [14] Hueso, R., et al. 2018. *Astron. Astrophys.* **617**, A68. [15] Čuk, M. et al. 2016. *Astrophys. J.* **820**, 97.